

MICROSTRUCTURE AND MECHANICAL PROPERTIES OF LOW DENSITY STEEL

**A THESIS SUBMITTED IN FULFILMENT
OF THE
REQUIREMENT FOR THE AWARD OF THE DEGREE**

**OF
MASTER OF TECHNOLOGY**

**In
Material Engineering
Metallurgical and Material Engineering Department**

Faculty of Engineering and Technology

**Jadavpur University
Kolkata-700032**

Session: 2020-2022

**BY
VIVEK KUMAR**

**Examination Roll No: M4MAT22007
Registration No: 154369 of 2020-2021**

UNDER THE GUIDANCE OF

**Dr. AMRITA KUNDU
Metallurgical and Material
Engineering Department
Jadavpur University
Kolkata-700032**

**Prof. SHIV BRAT SINGH
Metallurgical and Material
Engineering Department
Indian Institute of Technology
Kharagpur-721302 West Bengal**

JADAVPUR UNIVERSITY

2022

**FACULTY OF ENGINEERING AND
TECHNOLOGY**

**Department of Metallurgical and Material
Engineering**

Declaration of Originality and Compliance of Academic Ethics

I hereby declare that the work “**Microstructure and Mechanical Properties of Low Density Steel**” Contains literature survey and original research work by the undersigned candidate, as a part of his Master of Technology in Material Engineering studies. All information in this document have been obtained and presented in accordance with academic rules and ethical conduct. I also declare that, as required by these rules and conduct. I have fully cited and referenced all material and results that are not original to this work.

Place: Kolkata
Date: 16-08-2022

VIVEK KUMAR
Examination Roll No: M4MAT22007
Registration No: 154369 of 2020-2021

CERTIFICATE

This is to certify that the thesis entitled, “**Microstructure and Mechanical Properties Of Low Density Steel**” being submitted by **Vivek Kumar** for the award of the degree of Master of Technology (Material Engineering) of Jadavpur University, is a record of bonafide research work carried out of him under my supervision and guidance Mr. Vivek Kumar has worked for more than one year on the above problem at the department of the Metallurgical and Material Engineering Jadavpur University Kolkata and this has reached the standard fulfilling the requirements and the regulation relating to the degree

The contents of this thesis, in full or part, have not been submitted to any other university or institution for the award of any degree or diploma.



.....

(ADVISOR)

Dr. Amrita Kundu

Metallurgical and Material
Engineering Department,
Jadavpur University, Kolkata-700032

.....

(ADVISOR)

Prof. Shiv Barat Singh

Metallurgical and Material
Engineering Department,
IIT Kharagpur, West Bengal
-721302

.....

Prof. Pravash

Chandra Chakraborti

Head of the Department
Metallurgical and Material
Engineering Department,
Jadavpur University, Kolkata-700032

.....

Prof. Chandan Mazumdar

Dean:- Faculty of Engineering
and Technology (FET)
Jadavpur University Kolkata-700032

Certificate of Approval

The thesis is hereby approved as a creditable study of an engineering subject carried out and presented in a manner satisfactory to warrant its acceptance as a prerequisite to the degree for which it has been submitted. It is understood that by this approval the undersigned do not necessarily endorse or approve any statement made opinion expressed or conclusion drawn therein but approve the thesis only for the purpose for which it is submitted.

.....

(SIGNATURE OF EXAMINNERS)

**COMMITTEE ON FINAL EXAMINATION FOR EVALUATION
OF THE THESIS**

Acknowledgement

The satisfaction and euphoria that accompany the successful completion of a task would be incomplete without the mention of the people who made it possible and whose constant guidance and encouragement crowned all the efforts with success. Therefore, I would like to take this opportunity to express my sincere and heartfelt gratitude to all those who made this report possible.

At first I would like to thank My Guide, Thesis supervisor **Dr. Amrita Kundu**, Department of Metallurgical & Material Engineering, Jadavpur University. Without her support and invaluable guidance, it is impossible for me to complete this thesis.

I express my sincere gratitude to **Prof. Shiv Brat Singh**, Department of Metallurgical & Materials Engineering IIT Kharagpur and **Mr. Rahul Kumar Singh**, Research Scholar, Department of Metallurgical & Material Engineering, Jadavpur University, for their kind support in correcting my mistakes and giving useful suggestions. I like to acknowledge **Prof. Pravash Chandra Chakraborti**, Head, Metallurgical and Material Engineering Department for the provision of the research facilities.

I am also grateful to **Mr. Jayanta Bhattacharya**, Senior laboratory technician, Department of Metallurgical & Material Engineering, Jadavpur University, for encouraging, providing research facilities, helping me in analyzing data and supporting during this investigation.

My sincere regards to my friends at Jadavpur University like **Sonal Kumar Singh, Suraj Kumar, Tushar Das** and **Pratik Raj** for their co-operation during the period of work.

At last but not the least I thank my Parents and Family Members without whom support and motivation I cannot complete this work.

Vivek Kumar

M.Tech. (Metallurgical & Material Engineering)

CONTENTS

LIST OF FIGURES	8
ABSTRACT	9
CHAPTER-1	10
1.1 BACKGROUND AND MOTIVATION	10
1.2 OBJECTIVE.....	10
CHAPTER-2	11
LITERATURE REVIEW	11
2.1 INTRODUCTION	11
2.2 MICROSTRUCTURE BASED CLASSIFICATION	
OF LOW-DENSITY Fe-Mn-Al-C STEELS.....	12
2.3 MICROSTRUCTURE EVOLUTION IN LOW DENSITY	
STEELS.....	12
2.4 MICROSTRUCTURE EVOLUTION IN FERRITIC Fe-Mn-Al-C STEELS.....	12
2.5 MICROSTRUCTURAL EVOLUTION IN AUSTENITIC Fe-Mn-Al-C STEELS.....	13
2.6 MICROSTRUCTURE EVOLUTION IN DUPLEX Fe-Mn-Al-C STEELS.....	15
2.7 APPLICATION AND PROPERTIES OF LOW DENSITY STEELS.....	16
2.8 PHYSICAL PROPERTIES OF LOW DENSITY STEELS.....	16
2.9 MECHANICAL PROPPERTIES OF LOW DENSITY STEEL.....	18
CHAPTER-3.....	20
MATERIALS AND EXPERIMENTS	20
3.1 MATERIALS AND THEIR COMPOSITION.....	20
3.2 MICROSTRUCTURAL INVESTIGATION.....	20
3.3 TENSILE TEST.....	20
CHAPTER-4.....	21
RESULTS AND DISCUSSIONS	21
4.1 MICROSTRUCTURE IMAGES OF STEEL ALLOY.....	21
4.2 TENSILE PROPERTIES OF 10005 STEEL.....	24
4.2.1 ENGINEERING STRESS-STRAIN BEHAVIOUR.....	24

4.3 FRACTURE SURFACE ANALYSIS OF 10005 STEEL.....	25
4.3.1 SEM FRACTURE SURFACE IMAGES OF 10005 STEEL.....	25
CHAPTER-5.....	28
CONCLUSIONS AND SUGGESTIONS FOR FUTURE WORK.....	28
5.1 CONCLUSIONS.....	28
5.2 SUGGESTIONS FOR FUTURE WORK.....	28
REFERENCES.....	29

LIST OF FIGURES

Fig.2.1. κ -carbide distribution in a Fe-30.4Mn-8Al-1.2C austenitic steel annealed at 600°C for 24 h.

Fig.2.2. Bright-field TEM image of κ -carbides along the grain boundary between two adjacent austenitic grains γ_1 and γ_2 in a Fe-30.5Mn-8Al-1.2C austenitic steel annealed at 600°C for 96 h.

Fig.2.3. Optical micrograph of the banded structure of a ferrite-based duplex Fe-3.5 Mn-5.8Al-0.35C steel;44) (b): EBSD phase map of a hot-rolled austenite-based duplex Fe-8.5Mn-5.6Al-0.3C steel;47) (c): Bright-field TEM image of a Cu-rich B2 precipitate in a Fe-12Mn-7Al-0.5C-3Cu annealed at 830°C for 1 minute and strained to 0.02 [12].

Fig.2.4. Effect of alloy elements on the physical properties of ferritic iron:-Density reduction of ferritic iron by elements lighter than Fe [24,27];

Fig.2.5. The reduction of Young's modulus of Fe-Al steels in the annealed state as a function of Al content [24,28].

Fig.4.1. Microstructure of 10005 Steel.

Fig.4.2. Microstructure of 9183 Steel

Fig.4.3. Microstructure of 10006 Steel

Fig.4.4. Microstructure of 10007 Steel.

Fig.4.5. Microstructure of 10013 Steel.

Fig.4.6. Microstructure of 10060 Steel.

Fig.4.7. Tensile stress strain plots of 10005 Steel using different strain rates.

Fig.4.8. SEM fracture surface of 10005 Steel.

Fig.4.9. SEM fracture image of 10005 Steel

ABSTRACT

The Microstructural evolution, physical and mechanical properties of different types of Fe-Mn-Al-C low density steels has been discussed in literature review. It exhibits an excellent combination in mechanical properties, with a tensile strength of 846MPa and a total elongation of 32%.

The Focus of this study has been to investigate the microstructural analysis of different types of low density steels. Tensile behaviour of low density steel at different strain rates of $1 \times 10^{-1} \text{ s}^{-1}$, $1 \times 10^{-2} \text{ s}^{-1}$, $1 \times 10^{-3} \text{ s}^{-1}$ and $1 \times 10^{-4} \text{ s}^{-1}$ were examined and fracture surface imaging was carried out with scanning electron microscope.

CHAPTER-1

1.1 BACKGROUND AND MOTIVATION

The Fe-Mn-Al-C system was initially used in reports from the 1930s [1], which is when the term "low-density steels" originally appeared. After that, in the 1950s, [2] it became possible to substitute less expensive Mn and Al for more expensive Ni and Cr in stainless steels, hence improving the density. As less expensive alternatives to stainless steels and Ni-based superalloys, Fe-based aluminides FeAl and Fe₃Al were exhaustively studied during the 1980s and 1990s [3–10], while work on the previously described substitution of Ni and Cr in stainless steels was continued [11–12].

However, significant work on comprehending and creating low-density steels for use in automotive applications has just lately come to light. If other design requirements are met, it is advantageous to reduce the weight of an engineering structure since it saves resources and energy. Light metals like aluminium, magnesium, titanium, and their alloys are taken into consideration in preference to steels in order to accomplish this purpose. Steels, on the other hand, represent a relatively large volume in the production and usage of engineered materials globally. Steels are widely used in one of the major industrial sectors, the automotive industry, due to its great mix of strength, formability, recyclability, and most importantly, affordability. However, unfortunately, due to their high density (7.85 g cm³ for ferrite and 8.15 g cm³ for austenite), steels are not so effective in light-weighting of automotive structures, although as a result of increased strength, newer designs have succeeded in reducing the weight of the auto body and other components.

Additionally, even while they contribute significantly to the economies of developed nations (e.g., 3–3.5% of the GDP in the USA) [13], automobiles are also one of the world's main producers of greenhouse gas emissions, which is why they are subject to strict environmental restrictions [14]. In order to reduce carbon dioxide emissions and improve fuel efficiency, automobile vehicles must become lighter. Many different high-strength steel types can be used in vehicle parts with lower gauge, which results in weight savings. The development of special steels with lower density has recently received funding for various research initiatives [14–17]. The low-density steels usually include substitutional light element aluminum. The addition of aluminum as a strong ferrite stabilizer resulted in some δ -ferrite persisted in all the temperature range after solidification.

1.2 OBJECTIVES

The thesis is focused on examination of microstructure and mechanical properties of Low-density steels. The objective of the present investigation is aimed at evaluating the microstructure, tensile behaviour and fracture behaviour of the low density steel.

CHAPTER-2 LITERATURE REVIEW

2.1 INTRODUCTION

In recent years, researchers have paid great attention to Fe–Mn–Al–C series low density steel for its high strength and light weight to better achieve the developmental goal of energy conservation and emission reduction. This tendency has taken place in a number of industrial production sectors, such as transportation vehicles, maritime, oceanic submarines and aerospace [1–5]. As seen in most of the studies [6], the density of steel could be reduced by 1.3% per 1% Al. In addition, low-density steel is easily affected by various mechanisms, including transformation-induced plasticity (TRIP), twinning-induced plasticity (TWIP), shear band-induced plasticity (SIP), and microband-induced plasticity (MBIP) when subjected to external forces during use [6–9], which provides high strength and ductility at the same time. Low-density steel usually has high strong plastic product, the strong plastic product of Fe-30.5Mn-2.1Al-1.2C low-density steel developed by the Max Planck Metal Institute of Germany can reach 88GPa·% [10]. It has also been observed that the microstructure of low-density steel is affected by alloying elements. On one hand, the Mn element in low-density steel plays a role of solid solution strengthening [11], and on the other hand, Mn can also play a role in improving the stability of austenite. Similarly, Ni is also an austenite stabilizing element, which can improve toughness. Higher C content can improve the stability of austenite and enable low-density steel to obtain more retained austenite at room temperature [12], and Al shrinks the γ region and promotes the formation of ferrite [13]. Although Mn and C elements would expand the γ phase region, lesser amounts of Al elements also lead to the appearance of ferrite in the microstructure [14]. It is also noted that ferrite contains brittle phase δ -ferrite. Large amounts of Mn, Al, and other elements are added to low-density steel, which invites obvious segregation during the process of metal smelting. Therefore, it is difficult to guarantee the structure of low density steel as a single austenite in actual production. κ -carbide precipitates by spinodal decomposition and may precipitate both at grain boundaries and inside grains, so that the morphology and distribution of κ -carbide have a great influence on the mechanical properties of low-density steels. It has been seen that the effect of precipitation on the mechanical properties of low-density steel was mainly reflected in hot working. Fe–Mn–Al–C Low-density steels must contain a large amount of Al for weight reduction requirements.

For use in the automotive, chemical, and aircraft sectors, low density Fe–Mn–Al–C steels are one of a new class of structural materials. Due to the high Al concentration, these steels offer weight reductions of up to 18% while exhibiting exceptional tensile mechanical performance at both room temperature and cryogenic temperatures (1.3% density reduction for every addition of 1 weight percent of Al) [15]. These steels additionally possess desirable qualities such strong energy absorption behaviour, high strength and toughness at room and low temperatures, good fatigue resistance, and good oxidation resistance at rising temperatures [16-27]. In the last decade, low density Fe–Mn–Al–C steels have attracted considerable attention as these steel grades can potentially be used for lightweight crash-resistant car body structures and structural components in the cryogenic industry. Owing to the occurrence of several disordered and ordered fcc and bcc phases, Fe–Mn–Al–C steels exhibit outstanding combination of mechanical and physical properties that can be tuned by selective microstructural control. [16,19,22,24,25,28,29].

2.2 MICROSTRUCTURE-BASED CLASSIFICATION OF LOW-DENSITY Fe–Mn–Al–C STEELS.

Depending on the temperature and relative concentrations of alloying metals like Al, C, and Mn, the matrix phase of low-density steels can either be ferrite, austenite, or a mixture of ferrite and austenite. Lightweight Fe-Mn-Al-C alloys can be divided into four groups based on the matrix phases at high (hot working) temperatures, where it is assumed that equilibrium conditions are approaching: (1) ferritic steels [34–40], (2) ferrite based duplex steels [41–60], (3) austenite based duplex steels [61–70], and (4) austenitic steels [71–87]. Note that in this study, ferrite precipitated from austenite is referred to as δ -ferrite while ferrite formed from the liquid phase is referred to as α -ferrite. The δ -ferrite has different elemental composition/partitioning and intrinsic chemical gradients from the α -ferrite although they have the same crystal structure (BCC). Ferritic Fe–Al low-density alloys can contain up to 5% Mn but only a very low amount of C.

Austenitic low-density steels contain a higher Mn content, typically between 12 and 30%, Al up to 12% and C between 0.6 and 2.0%. This type of alloys can have a fully equiaxed-austenitic microstructure at hot working temperatures and the austenite is metastable after fast cooling. Ferrite based duplex low-density steels have a microstructure of $\gamma + \delta$ -ferrite at hot working temperature, with the fraction of the δ -ferrite being larger than 50%. The stability of the austenite is relatively low because of the lower amounts of alloying elements. Because of the large difference in the C and Mn contents and also the difference in the processing parameters, this family of alloys may represent different and complex transformation behaviours at lower temperatures. Austenite based duplex low density steels have a microstructure of $\gamma + \delta$ at hot working temperature with the austenitic phase forming the continuous matrix. The stability of the austenite is quite high because of the higher amounts of alloying elements. The austenite may stabilize to the room temperature, along with κ -precipitation forming inside the austenite grains.

2.3. MICROSTRUCTURE EVOLUTION IN LOW DENSITY STEELS.

2.3.1. Microstructural Evolution in Ferritic Fe–Mn–Al–C Steels

As a result of the ferritic Fe-Al steels' high Al content and low C content throughout the whole process temperature range. The ferrite phase, or δ -ferrite, was created during the casting process directly from liquid. In the single ferrite phase range, hot working has been performed. The grain size of the δ -ferrite cannot be sufficiently refined through dynamic recrystallization during hot rolling or static recrystallization between the hot rolling passes under the usual hot rolling conditions for HSLA steels because Al not only extended the ferrite region at high temperatures, but also raised the recrystallization temperature of ferrite. In the subsequent cooling process, coarse κ -carbides could be formed along the original δ -ferrite grain boundaries if the cooling rate was slow [39–43]. It was observed that the κ -carbides in ferritic matrix are semi coherent and in the form of thick and elongated rod-like shape [59]. In most of the investigations it was mentioned that Cold rolling and annealing are necessary steps to change the grain structure, grain size and texture in ferritic low density steels [37–43].

2.3.2. Microstructural Evolution in Austenitic Fe-Mn-Al-C Steel.

High Mn concentration (15-30 wt%), Al content of 2–12 wt%, and high C content (0.5–2.0 wt%) are characteristics of austenitic Fe–Mn–Al–C steels. The fully equiaxed austenitic microstructure of these low-density steels was visible under hot working conditions. The pace of cooling and the contents of Al and C affected the behaviour of carbide precipitation and the properties of the $\gamma \rightarrow \alpha$ transformation. High Al content (> 9 wt%) in particular encouraged the development of disordered ferrite with organised B2 and DO₃ domains along grain boundaries [9]. Although other carbides, such as M₂₃C₆, M₇C₃, and M₃C, has also affected the mechanical performance, from a mechanical aspect, κ -carbides (L1'2 phase) are the most significant precipitates in these **steels**. It has been observed that the formation of κ -carbides in austenitic Fe–Mn–Al–C steels requires high Al and C contents, namely Al > 5 wt.% and C > 1 wt.% (Fig.1). κ -carbides are coherent or semi coherent precipitates (lattice misfit $< 2\%$) with a cube-on-cube orientation relationship with austenite. carbide distribution consists of a complex three-dimensional arrangement of cuboidal and plate-like precipitates with diameter of about 10–50 nm along the three orthogonal $\langle 001 \rangle$ directions. 2-D analysis of κ -carbide distribution by TEM typically shows a side band distribution of nanosized precipitates along directions, Fig.2.1 shows the [15] 3-D analysis of κ -carbide distribution by atom probe tomography (APT) has recently revealed that κ -carbides are compactly distributed into stacks with different inter-particle. By spinodal breakdown, or chemical manipulation, of the metastable γ -phase followed by ordering, κ -carbides can be massively precipitated in austenitic Fe-Mn-Al-C steels (volume percentage up to 40%). The κ' -phase has the same crystal structure as the κ -phase, but the C atoms' occupation is incomplete. With an increase in Al and C contents, particularly when Al $> 10\%$ and C $> 1\%$, the kinetics of spinodal breakdown and the density of κ -carbides also increased. Prolonged aging in the temperature range 450–650°C results in the increase of the lattice parameter of κ -carbide and the decrease of that of austenite. This effect promotes the loss of coherency of κ -carbides. At annealing temperatures of 650–800°C, coarse κ -carbides tend to precipitate along grain boundaries resulting in lamellar γ/κ structure, Fig.2.2 Depending on steel composition and annealing conditions, these carbides can be formed through different types of reactions such as cellular transformations and eutectoid reactions [28,30,41]. It was found that Grain boundary κ -carbides have parallel orientation relationship with one of the neighbouring grains. At the early precipitation stages, κ -carbides were formed as discrete particles along grain boundaries. With further annealing in the $(\gamma + \kappa)$ or the $(\gamma + \alpha + \kappa)$ regions, these carbides transformed into thin films distributed continuously along grain boundaries that grew into adjacent grains, High temperature (800°C) aging of austenitic Fe–Mn–Al–C steels with high content resulted in the $\gamma \rightarrow \alpha$ transformation [32]. It was seen that the resulting ferrite phase contains ordered B2 and DO₃ structures, which are detrimental to mechanical performance.

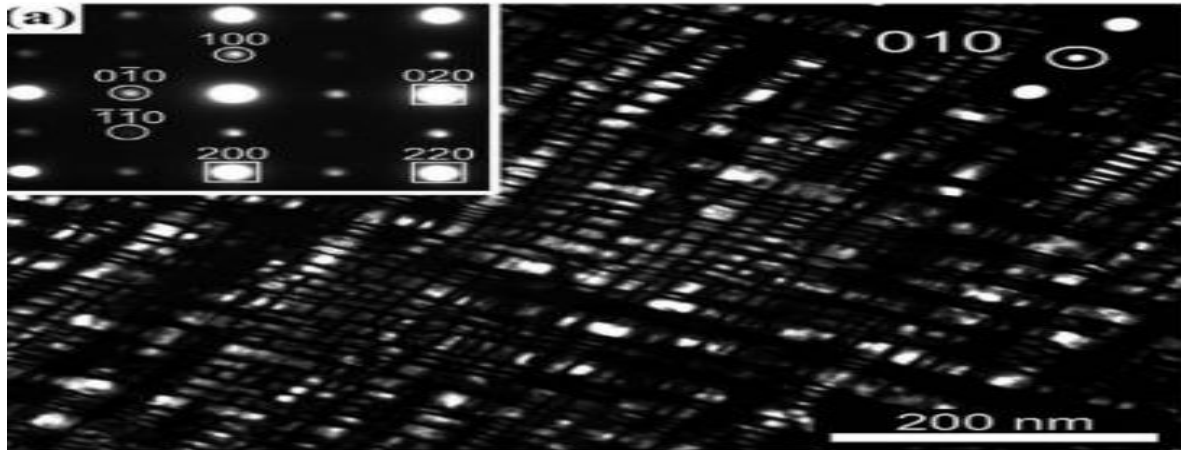


Fig 2.1 κ -carbide distribution in a Fe-30.4Mn-8Al-1.2C austenitic steel annealed at 600°C

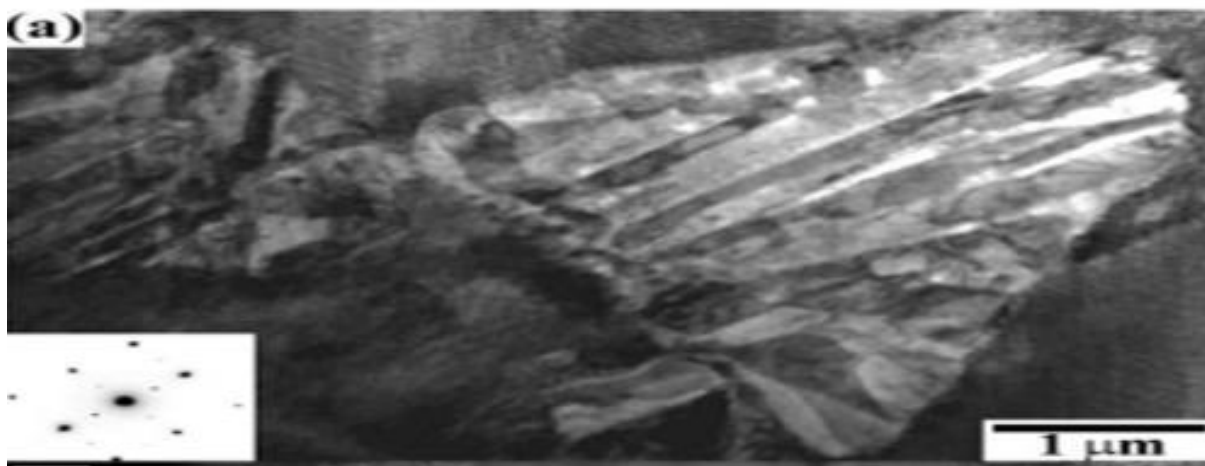


Fig.2.2 Bright-field TEM image of κ -carbides along the grain boundary between two adjacent austenitic grains γ_1 and γ_2 in a Fe-30.5Mn-8Al-1.2C austenitic steel annealed at 600°C for 96 h [33].

2.3.3 Microstructural Evolution in Duplex Fe–Mn–Al–C Steels.

A complicated multiphase microstructure composed of δ -ferrite, α -ferrite, austenite, and κ -carbides distinguishes duplex Fe–Mn–Al–C steels from other types of steel. Ferrite-based duplex steels with a high Mn concentration can produce α' -martensite and bainite. The solidification microstructure during the hot rolling process featured macroscopic segregations of these elements as a result of the high alloying concentrations of Mn and Al, creating a macroscopic banded structure. The structure, size, volume fraction, and distribution of the structural phases can be controlled by adjusting the thermo mechanical conditions. From the standpoint of matrix phase structure, low density duplex steels can be classified into ferrite- and austenite-based duplex steels. The microstructural features of these steels are the following. Ferrite-based duplex steels contain medium Mn content (3–10 wt.%), Al content of 5–9 wt.% and low C content (< 0.4 wt.%) [10,44,48]. It has been investigated that these steels are characterized by a complex bimodal banded structure of δ -ferrite and austenite bands elongated along the rolling direction as shown in Fig.2.3(a). It has been observed that the phase structure of the austenite band is strongly dependent on the Mn content and annealing treatment. Austenite partially or completely transformed into lamellar colonies of ($\alpha + \kappa$) that were formed along the parent γ -grain boundaries or at δ/γ interfaces. The lamellar ($\alpha + \kappa$) structure can be characterized by elongated rod-like semi coherent κ -carbides. At high Mn content, the decomposition $\gamma \rightarrow \alpha + \kappa$ was suppressed and the martensitic transformation $\gamma \rightarrow \alpha'$ occurred [46,47]. Austenite-based duplex steels contain high Mn content (10–25 wt.%), Al content of 5–12 wt.% and C content of 0.6–1.2 wt.%. [3,8,9,11,12,32,43,45,47,49,50]. Fe–Mn–Al–C steels with high Mn and Al contents (Mn > 25 wt.% and Al > 9 wt.%) can exhibit fully austenitic structure in the as-quenched state. Upon further aging at 500–800°C, complex ferritic band structure can be formed along austenitic grain boundaries. On the other hand, ferrite-based duplex steels are characterized by a complex bimodal banded structure of δ -ferrite and austenite bands elongated along the rolling direction, Fig 2.3(b). As this figure shows, austenite can undergo strain induced α' -martensitic transformation. Together with the formation of L'12 κ -carbides, several precipitation strategies have been recently suggested to promote the formation of ordered B2-type precipitates. Additions of Ni and Cu of around 3–5 wt.% enable the formation of non shearable B2-type precipitates in austenitic bands resulting in enhanced mechanical performance [8,12,50]. As an example, Fig.2.3(c) shows the piling-up of dislocations at the interface of a B2 Cu-rich precipitate in a Fe-12Mn-7Al-0.5C-3Cu steel. Depending on the alloying content and annealing conditions, it can be said that ferritic bands contain B2 precipitates, κ -carbides, and austenite grains. κ -carbides are formed through the eutectoid decomposition $\gamma \rightarrow \alpha + \kappa$.

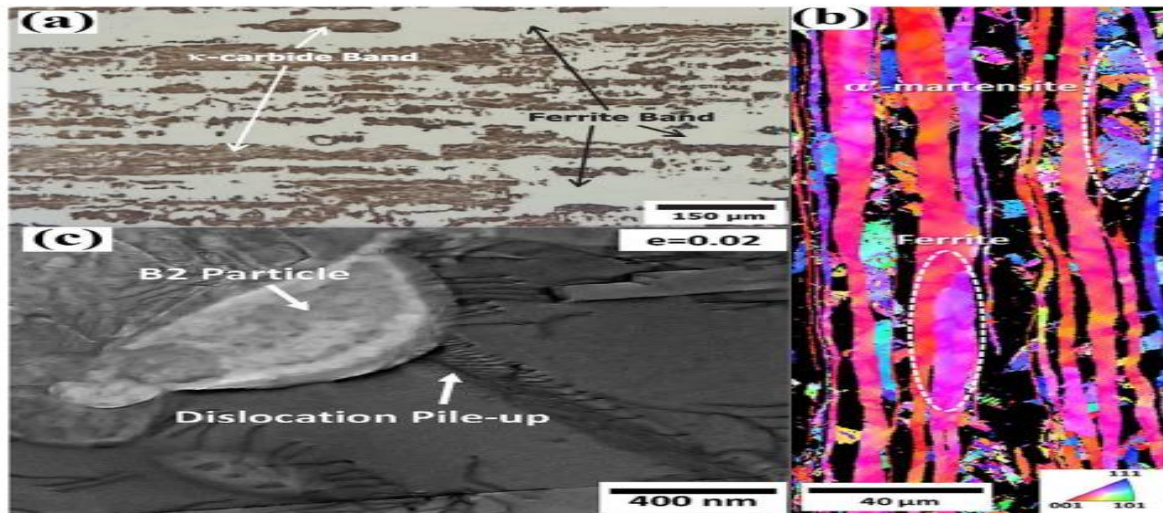


Fig.2.3(a): Optical micrograph of the banded structure of a ferrite-based duplex Fe-3.5 Mn-5.8Al-0.35C steel;44) (b): EBSD phase map of a hot-rolled austenite-based duplex Fe-8.5Mn-5.6Al-0.3C steel;47) (c): Bright-field TEM image of a Cu-rich B2 precipitate in a Fe-12Mn-7Al-0.5C-3Cu annealed at 830°C for 1 minute and strained to 0.02.[12]

2.4 APPLICATION AND PROPERTIES OF Fe-Mn-Al-C LOW DENSITY STEELS.

2.4.1 Physical properties of Fe-Mn-Al-C low density steels

Density:-

Most researchers found that the weight reduction is the main driving force for developing Fe-Mn-Al-C steels for automotive applications. Alloying elements with a lower density than Fe (7.8 g/cm^3) such as Al (2.7 g/cm^3), Si (2.3 g/cm^3), Mn (7.21 g/cm^3) and Cr (7.19 g/cm^3) can often be added to Fe-C steels to reduce the density as well as to control the phase constitution. It can be seen that light elements change the lattice parameter of steels and at the same time reduce density by virtue of their low atomic masses [24–26]. For Example, a 12% aluminium addition will reduce the density of iron by 17%. In Fig.2.4 the effects of alloying elements on density reduction in ferritic steels up to a maximum of 16% alloy content can be seen. It can also be deduced that the density of steel decreases linearly with increasing addition of the elements Al, C, Si and Mn. This indicated a 1.3% reduction in density per 1% Al addition. The addition of C is very effective in density reduction for austenitic low-density steels. The effectiveness of C is about four times higher than that of Al.

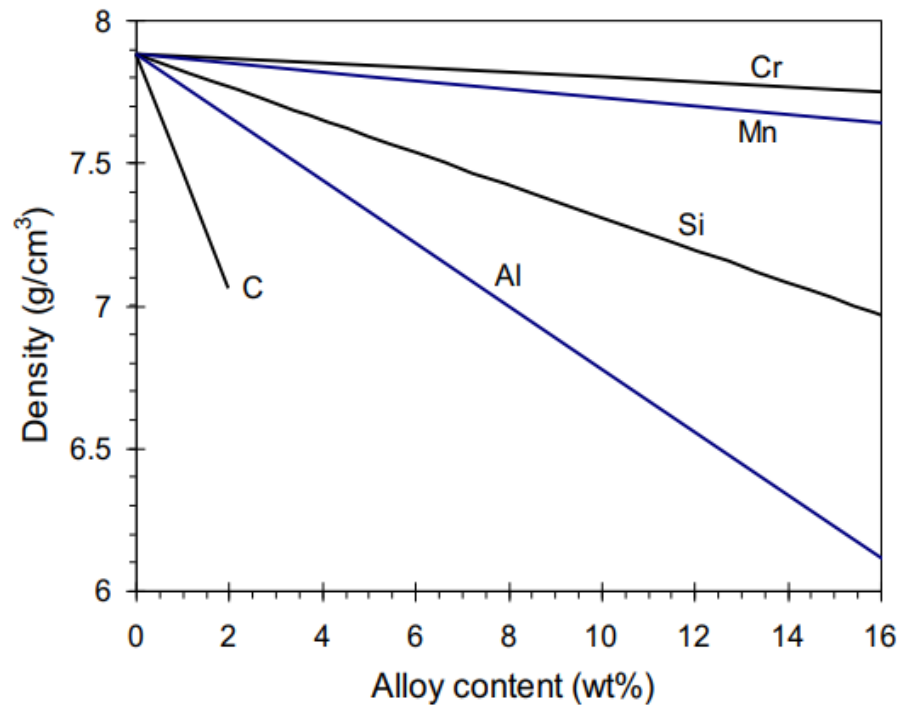


Fig.2.4. Density reduction of ferritic iron by elements lighter than Fe [24,27].

Young's modulus: -

It has been observed that an increase in the young's modulus (E modulus) improves the stiffness of automotive parts. It was found that one of the critical disadvantages of low-density steels is that the addition of Al decreases the Young's modulus. The elastic moduli of polycrystalline Fe-Al alloys in the annealed state at room temperature is a function of the Al content [24,28]. The collected data of the Young's modulus were measured with dynamic measurements such as the resonance method or the ultra-reduction in the Young's modulus per 1% Al addition is obtained. It was seen in most of the investigations that the decrease of the Young's modulus with increasing the Al content is caused by a reduction of lattice energy of the Fe-Al solid solution and the larger distance between coexisting Fe and Al atoms in the lattice [26]. Si and Cr are reported to slightly increase the E modulus of steels containing high amounts of Al, while Mn slightly decreases it [29]. As the micro-cavities were reduced during reheating and hot rolling it was seen that the Young's modulus was higher in the hot rolled state. Cold deformation does have a reducing influence on the Young's modulus [34 35]. As mentioned earlier, the weight saving potential of a low density steel depends on both the Young's modulus and density.

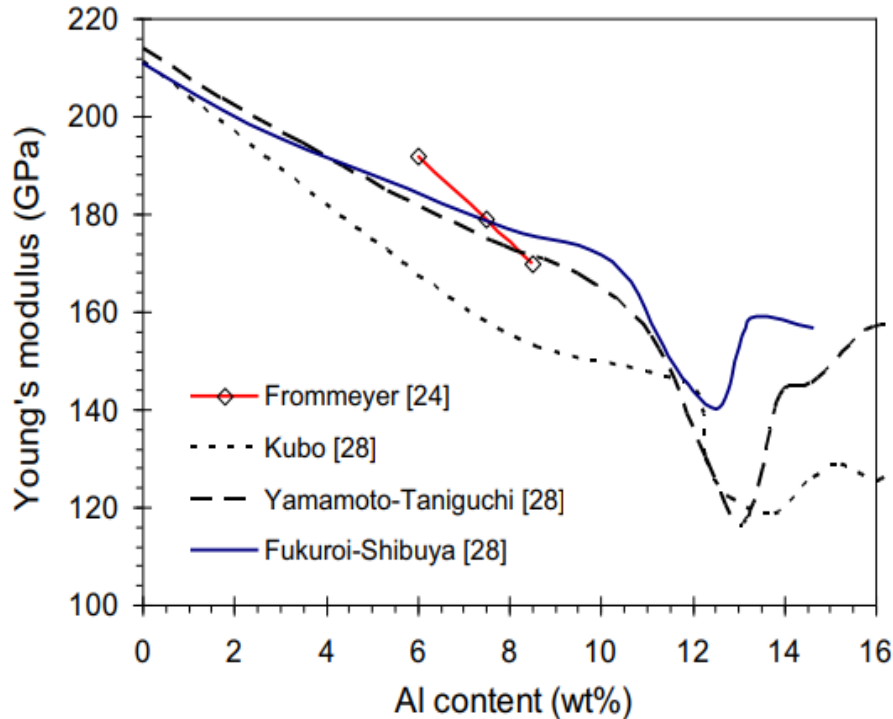


Fig.2.5. The reduction of Young's modulus of Fe-Al steels in the annealed state as a function of Al content [24,28].

2.4.2 Mechanical Properties of Low-Density Steels

Impact toughness:-

It can be observed for structural purposes, a good combination of mechanical strength and fracture toughness is desirable. Authors have studied the tensile properties and the impact toughness as a function of temperature in a Fe-30Mn-10Al-1C-1Si [71]. It can be seen that the impact toughness of Fe-Mn-Al-C steels depends on the phase constituents and their distributions, in particular, the formation of κ -carbides and the presence of δ -ferrite. It was also observed that when the Al content was below 7%, there was no κ -carbide formation but instead of κ -carbides, other carbides such as Fe_3C or M_7C_3 might have been produced along the grain boundaries during aging. The distribution of these carbides had little effect on the strength but reduced the ductility and toughness significantly. As Al was increased above 7%, Fe_3C or M_7C_3 carbides were retarded and κ -carbides formed. The strength increased but ductility and impact toughness decreased due to an increasing volume fraction of the hardening κ -carbide particles [71].

Fatigue behaviour:-

The fatigue behaviour of three solution-treated Fe-29Mn-9Al-(0.26, 0.6, 1.06) C alloys was studied by Chang et al. [11, 73]. Solution treatment was performed at 1050°C for 1.5 h. The volume fractions of austenite were 45%, 90% and 100%, respectively, with increasing the carbon content. All three alloys exhibit a similar cyclic life response under equal stress amplitude despite differences in microstructure and strength. It was observed in the as-quenched condition Fe-Mn-Al-C steels have higher fatigue strength than the austenitic Cr-Ni

steels, but are inferior to martensitic Cr steels. the fatigue crack growth (FCG) behaviour and elastic plastic fracture toughness (K_{IC} -integral) of an austenitic Fe-Mn-Al-C alloy, and they have shown that this alloy system offers better fatigue crack growth resistance, compared with the conventional 304L austenitic stainless steel.

Formability:-

Formability, which is important for automotive applications, it is the ability of a material to undergo the desired shape changes without necking failures. The normal anisotropy factor and the strain hardening exponent are usually considered the most important factors for sheet forming properties. In general, the full austenitic Fe-Mn-Al-C steels display a lower work-hardening rate compared with high Mn steels, although no report about the anisotropy value can be found.

Corrosion resistance:-

It can be found through the investigations that the corrosion resistance of Fe-Mn-Al-C alloys in aqueous environments is far inferior to that of 304 stainless steel [74,76] and is comparable to that of the conventional high strength steels [5]. Many researchers tried to improve the corrosion resistance of the austenitic Fe-Mn-Al-C alloys by adding Cr and decreasing C [75,76]. Fe-Mn-Al-Cr-C alloys with a greater Cr and a lower C are duplex (austenite + ferrite) steels, and their mechanical properties are drastically inferior to those of austenitic steels because Cr and C are ferrite and austenite formers, respectively [77,78]. Because pitting is the main kind of corrosion and preferentially occurred within the α grains and on the α/γ grain borders in duplex Fe-Mn-Al-C alloys, their corrosion resistance is poorer than that of austenitic Fe-Mn-Al-C alloys [79]. A correct ratio of Cr and C contents is required to achieve a fully austenitic structure. The stress corrosion cracking behaviour of Fe-Mn-Al-C alloys cannot be improved due to the addition of Al, which was expected to provide active protective function [79,80].

Weldability:-

Fe-28Mn-(5-6) Al-1C alloys were welded by electron-beam [81,82] and continuous wave CO₂ laser techniques [81]. The microstructure of the welded metals consisted mainly of the columnar dendrites with a preferred orientation and some equiaxed austenitic structures in the central portion of the weld pool. The growth and convergence of these columnar dendrites led to the formation of an apparent 'parting' in the weld centreline. The parting exhibited a lower hardness value while peak hardness was observed in the heat affected zone (HAZ) of the weld. The tensile and impact tests indicated that the weld materials exhibited lower tensile strength, lower elongation and lower impact energy than those of the base alloy.

CHAPTER-3

MATERIALS AND EXPERIMENTS

The materials under investigation are different types of low density steels. The chemical compositions, microstructures and basic material characterizations are described in this chapter. The study of tensile behaviour is the objective of present investigation. The fracture surface images are also presented.

3.1 MATERIALS AND THEIR COMPOSITIONS

The chemical compositions of the steels are given in the Table 1.

Table 1. **Steel compositions in wt. %**

Alloys	C	Al	Mn	Si
9183	0.179	6.57	3.34
10005	0.134	9.14	5.34
10006	0.04	9.74
10007	0.0066	6.78	1.5
10013	0.0035	6.81
10060	0.0015	8.1

3.2 MICROSTRUCTURAL INVESTIGATION

Optical microscopy through Leica optical microscope fitted with a digital camera is done to reveal the microstructure of the different types of steel alloy. Sample preparation is a vital part of optical microscopy which consists of cutting of the sample, mounting, polishing and etching respectively. Polishing is done until scratch free, smooth mirror like surface is obtained and then etching is done. Etching is needed to reveal the microstructure of the specimen by etching contrast. Etchant used to reveal the microstructure is 2% nital solution.

3.3 TENSILE TEST

All the mechanical tests were performed at room temperature ($\sim 25^{\circ}\text{C}$) in a computer controlled close loop servo-electric universal testing machine of ± 100 KN load capacity (Instron 8862). Tensile tests were performed with different strain rates of $1 \times 10^{-1} \text{ s}^{-1}$, $1 \times 10^{-2} \text{ s}^{-1}$, $1 \times 10^{-3} \text{ s}^{-1}$ and $1 \times 10^{-4} \text{ s}^{-1}$.

CHAPTER-4

RESULTS AND DISCUSSIONS

The microstructure analysis of different steels is discussed in section 4.1. Tensile behaviour of the material 10005 steel is presented and discussed in section 4.2 and fracture surface images of 10005 steel are also presented and discussed in section 4.3.

4.1 MICROSTRUCTURE ANALYSIS OF DIFFERENT STEELS

4.1.1 Microstructure images of different types of steel have been captured with the help of optical microscope.

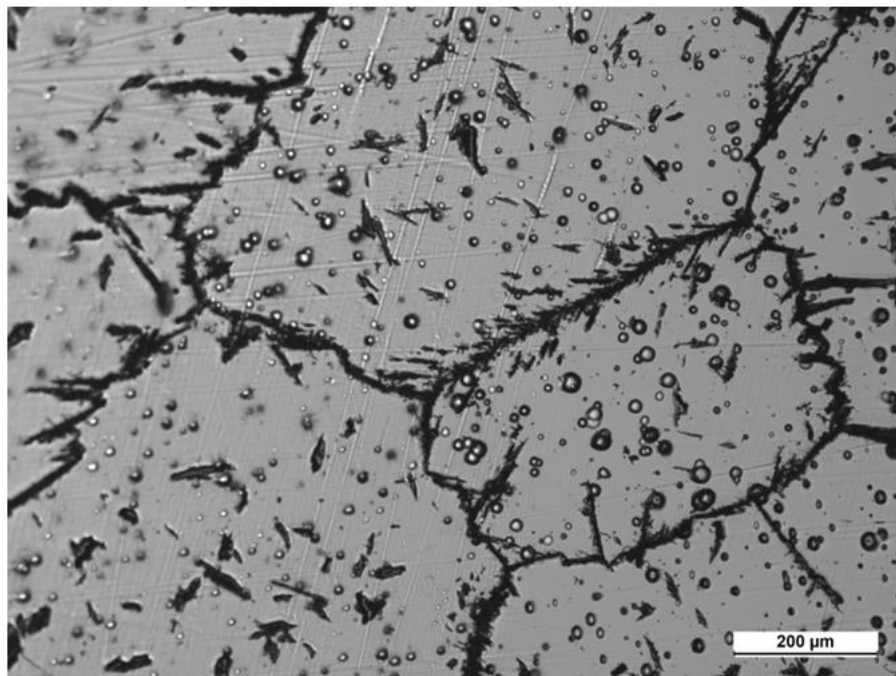


Fig.4.1. Microstructure of 10005 steel.

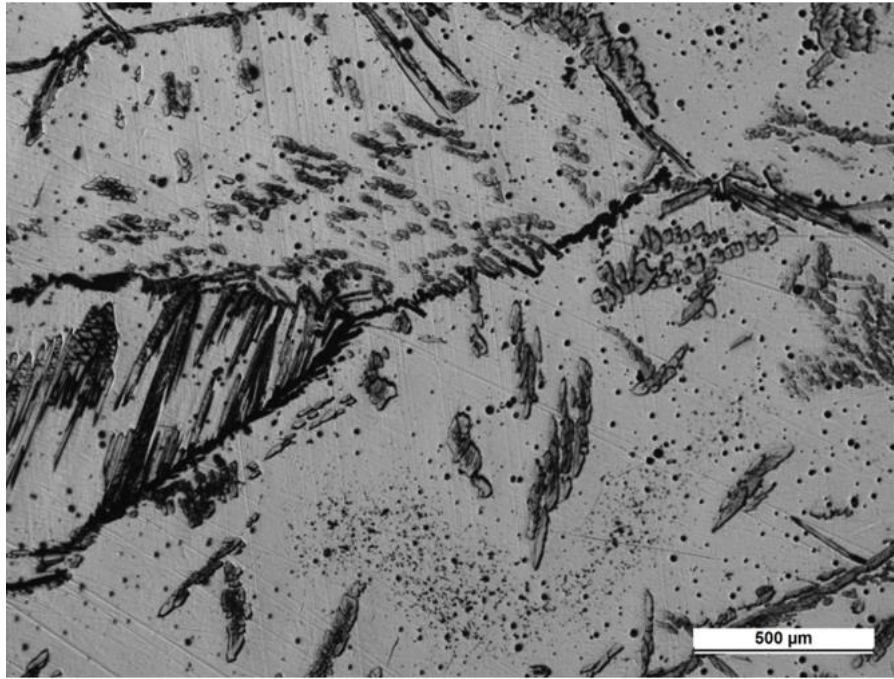


Fig.4.2. Microstructure of 9183 steel.

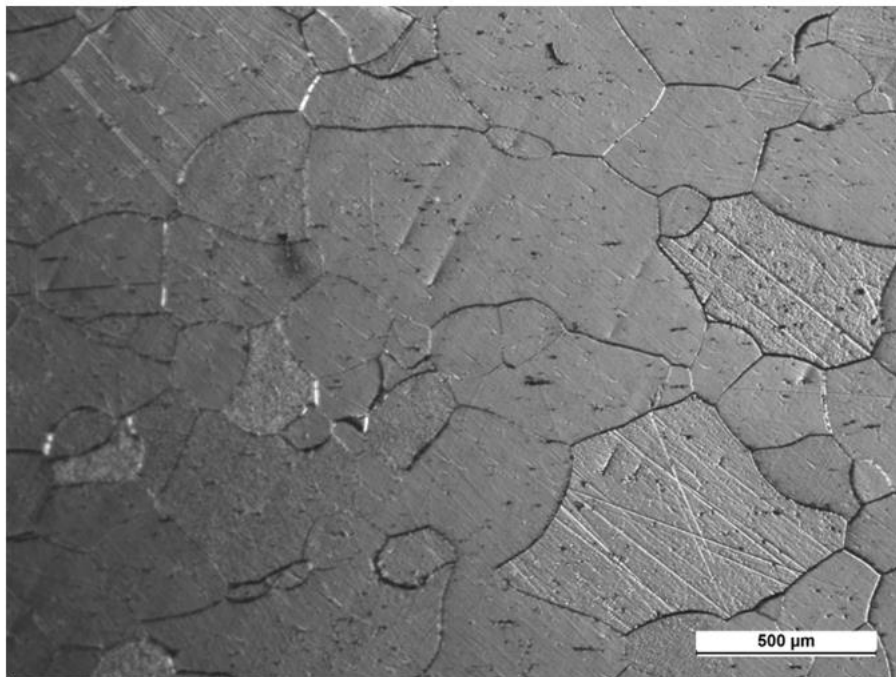


Fig.4.3. Microstructure of 10006 steel.

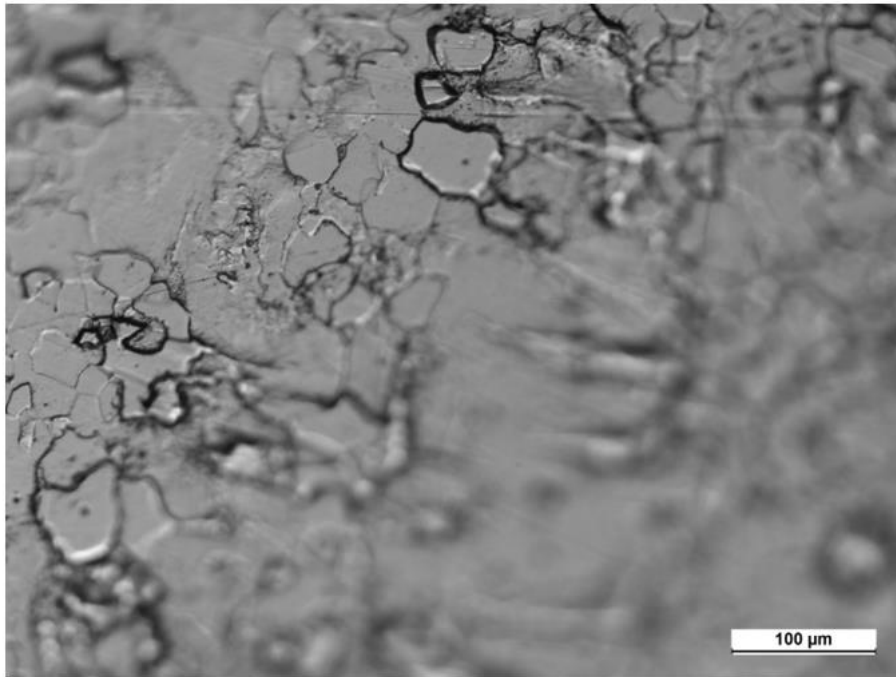


Fig.4.4. Microstructure of 10007 steel.

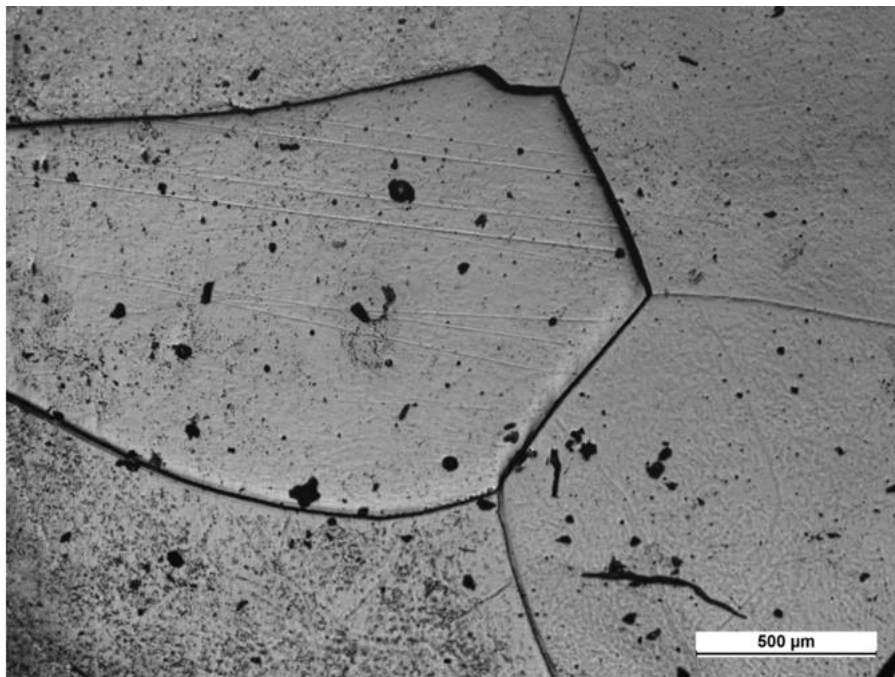


Fig.4.5. Microstructure of 10013 Steel.

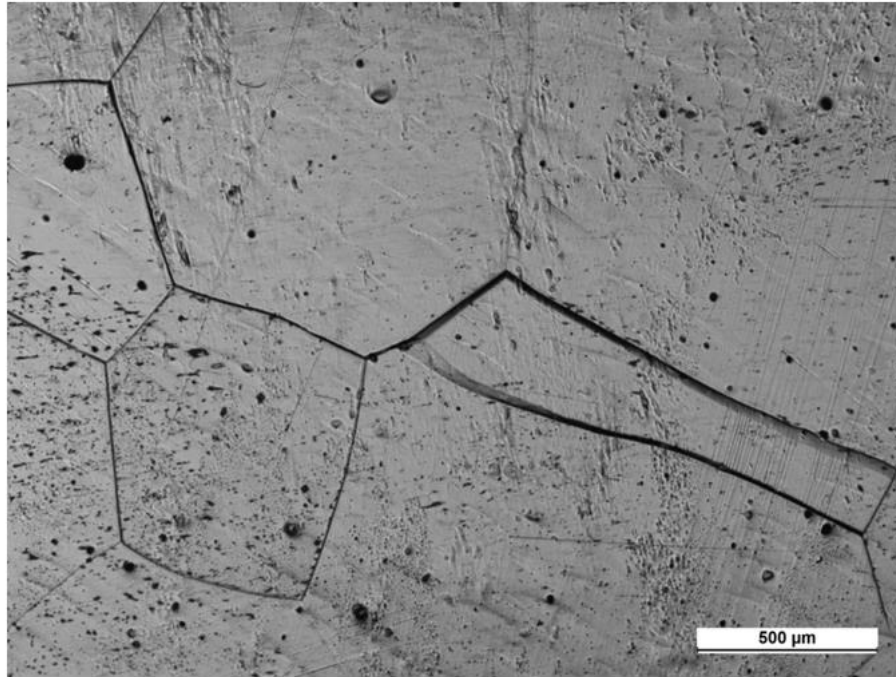


Fig.4.6. Microstructure of 10060 steel.

4.2 TENSILE PROPERTIES OF THE 10005 STEEL

4.2.1 Engineering Stress-strain Behaviour

Figure 4.7 shows the engineering stress-strain curve of the 10005 steel specimen at different strain rates. The tensile test results of 10005 steel shows that the 0.2% offset, different yield strength (YS) and ultimate tensile strength (UTS) at different strain rates.

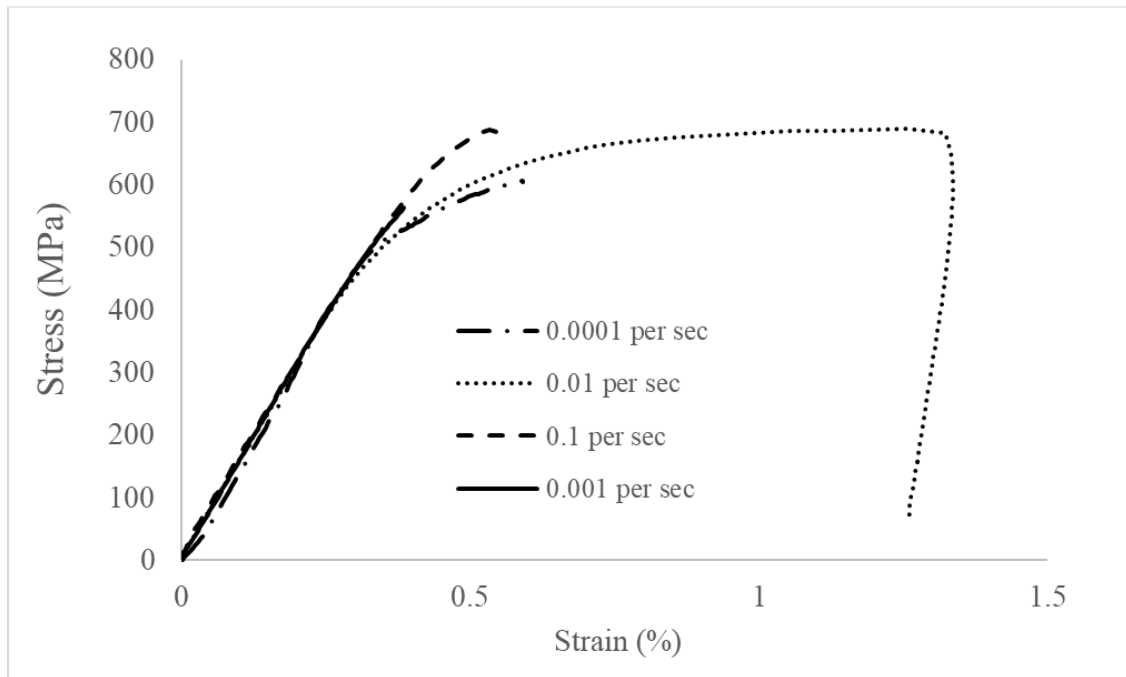


Fig.4.7. Tensile stress strain plots of 10005 steel using different strain rates.

4.3 FRACTURE SURFACE ANALYSIS OF 10005 STEEL

The fracture morphology of 10005 steel, which possesses the common features of cleavage fracture. There were some flat "class cleavage" facets, micro pores, tear edges, secondary cracks. The river pattern was short and curved with less tributaries, and the herringbone crack showed the direction of crack propagation.

4.3.1 To observe the fracture surface, SEM images of the 10005 steel specimen has been captured. The SEM fracture surface of 10005 steel specimen are given below.

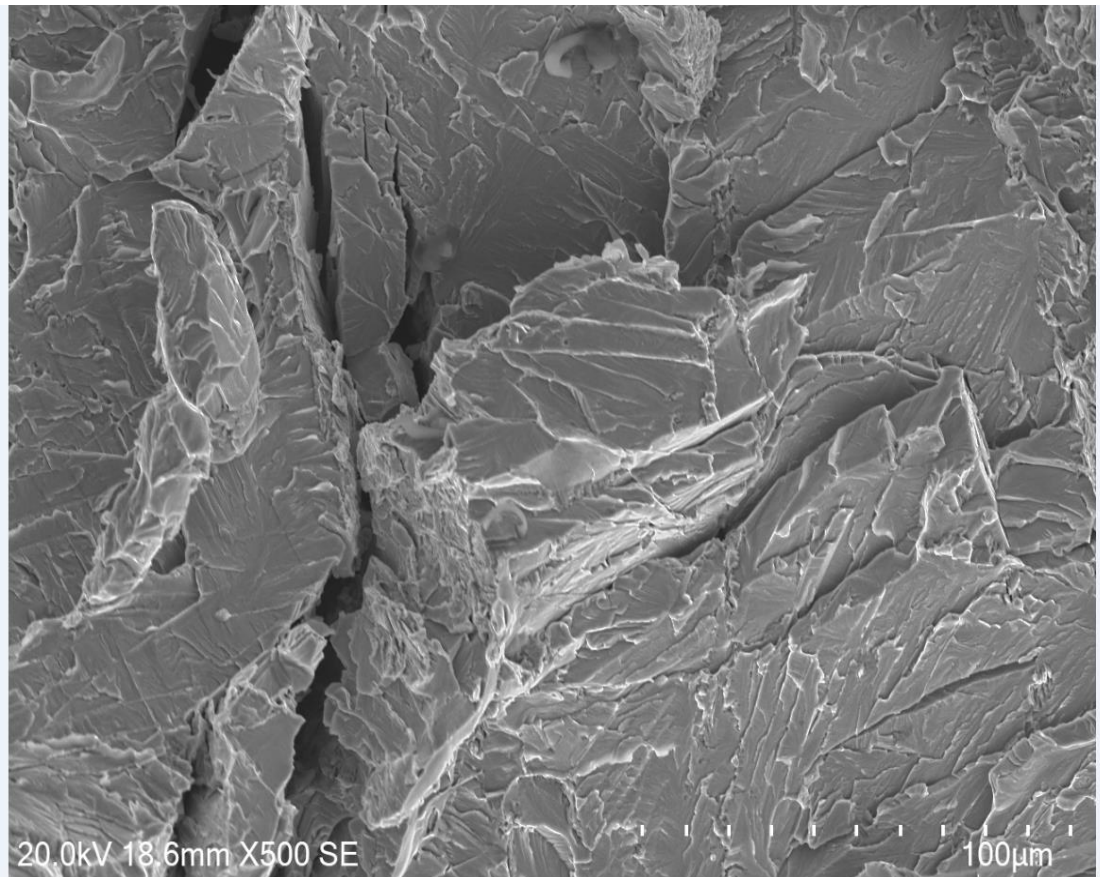


Fig.4.8. SEM fracture surface of 10005 steel specimen.

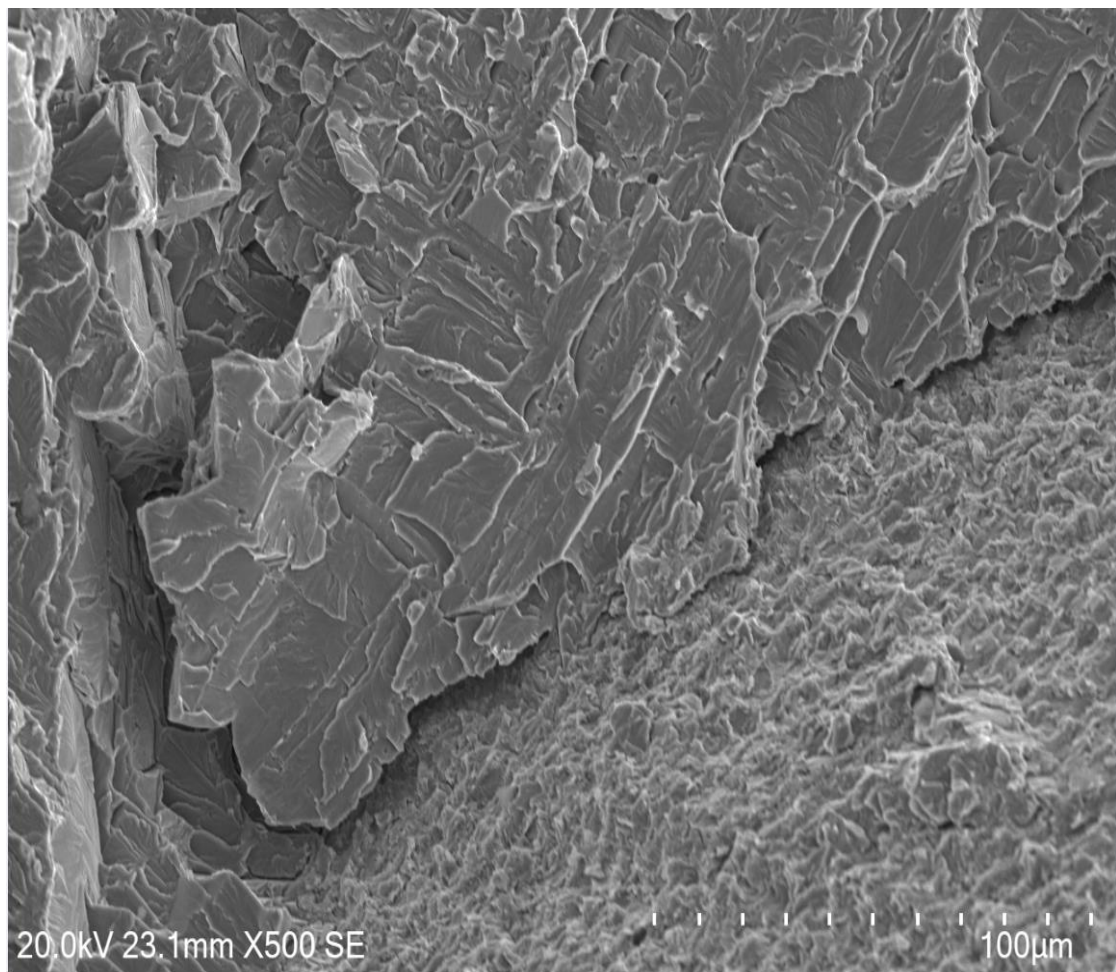


Fig.4.9. SEM fracture surface of 10005 steel specimen.

CHAPTER-5

CONCLUSIONS AND SUGGESTIONS FOR FUTURE WORK

5.1 CONCLUSIONS

The present thesis is an attempt to characterize the effect of microstructure on tensile properties at different strain rates.

Present investigation leads to following conclusions:

- The material behaves like brittle material as shown from figure of stress-strain curve.
- Yield stress is decreases as strain rate decreases.
- As shown in SEM image analysis, all the fracture occurred like cleavage facets which indicate lack of ability to accommodate the deformation.

5.2 SUGGESTIONS FOR FUTURE WORK

- New and innovative processing and manufacturing techniques must be developed.
- More test result required to explain the tensile and fracture behaviour of the specimen.
- The alloying and process strategies to improve the Young's modulus of the low-density steels should be explored.
- Fractographic analysis of 10005 steel need to investigated.

REFERENCES

- [1] Alu Matter (European Aluminium Association and MATTER), aluminium.matter.org.uk.
- [2] R. Rana, *Can. Metall* (2014).
- [3] K. Hill, D. Menk, and A. Cooper,
- [4] Regulation (EC) No 443/2009 of the European Parliament and of the Council (April 2009).
- [5] W. Korter and W. Ton, *Arch. Eisenhuettenw.* 7, 365 (1933).
- [6] J.L. Ham and R.E. Carin, *Prod. Eng.* 52, 59 (1958).
- [7] U. Prakash, R.A. Buckley, H. Jones, and C.M. Sellars, *ISIJ Int.* 31, 1113 (1991).
- [8] I. Baker and P.R. Munroe, *Int. Mater. Rev.* 42, 181 (1997).
- [9] C.G. McKamey, J.H. De Van, P.F. Tortorelli, and V.K. Sikka, *J. Mater. Res.* 6, 1779 (1991).
- [10] M.A. Van Ende, M. Guo, J. Proost, B. Blanpain, and P. Wollants, *ISIJ Int.* 51, 27 (2011).
- [11] M.L. Glenn, S.J. Bullard, D.E. Larson, and S.C. Rhoads, *J. Mater. Energy Syst.* 7, 75 (1985).
- [12] A.H. Bott, F.B. Pickering, and G.J. Butterworth, *J. Nucl. Mater.* 141–143, 1088 (1986).
- [13] D.-W. Suh and N.J. Kim, *Scr. Mater.* 68, 337 (2013).
- [14] R. Rana, C. Liu, and R.K. Ray, *Scr. Mater.* 68, 354 (2013)
- [15] D. Raabe, H. Springer, I. Gutierrez-Urrutia, F. Roters, M. Bausch, J.-B. Seol, M. Koyama, P.-P. Choi and K. Tsuzaki: *JOM*, 66 (2014), 1845.
- [16] K. Choi, C.-H. Seo, H. Lee, S. K. Kim, J. H. Kwak, K. G. Chin, K.-T. Park and N. J. Kim: *Scr. Mater.*, 63 (2010), 1028.
- [17] H. Ding, D. Han, Z. Cai and Z. Wu: *JOM*, 66 (2014), 1821.
- [18] G. Frommeyer and U. Brück: *Steel Res. Int.*, 77 (2006), 627.
- [19] I. Gutierrez-Urrutia and D. Raabe: *Acta Mater.*, 60 (2012), 5791.
- [20] I. Gutierrez-Urrutia and D. Raabe: *Scr. Mater.*, 68 (2013), 343.
- [21] H. Kim, D.-W. Suh and N. J. Kim: *Sci. Technol. Adv. Mater.*, 14 (2013), 014205.
- [22] S.-H. Kim, H. Kim and N. J. Kim: *Nature*, 518 (2015), 77.
- [23] K.-T. Park, S. W. Hwang, C. Y. Son and J.-K. Lee: *JOM*, 66 (2014), 1828.
- [24] S. S. Sohn, K. Choi, J.-H. Kwak, N. J. Kim and S. Lee: *Acta Mater.*, 78 (2014), 181.
- [25] S. S. Sohn, H. Song, B.-C. Suh, J.-H. Kwak, B.-J. Lee, N. J. Kim and S. Lee: *Acta Mater.*, 96 (2015), 301.

- [26] H. Song, J. Yoo, S.-H. Kim, S. S. Sohn, M. Koo, N. J. Kim and S. Lee: *Acta Mater.*, 135 (2017), 215.
- [27] S. Chen, R. Rana, A. Haldar and R. K. Ray: *Prog. Mater. Sci.*, 89 (2017), 345.
- [28] E. Welsch, D. Ponge, S. M. H. Haghighat, S. Sandlöbes, P. Choi, M. Herbig, S. Zaefferer and D. Raabe: *Acta Mater.*, 116 (2016), 188.
- [29] M. J. Yao, E. Welsch, D. Ponge, S. M. H. Haghighat, S. Sandlobes, P. Choi, M. Herbig, I. Bleskov, T. Hickel, M. Lipinska-Chwalek, P. Shanthraj, C. Scheu, B. Gault and D. Raabe: *Acta Mater.*, 140 (2017), 258.
- [30] Chao CY, Liu CH. Effects of Mn contents on the microstructure and mechanical properties of the Fe–10Al–xMn–1.0C alloy. *Mater Trans* 2002.
- [31] Salak A. *Ferrous powder metallurgy*. Cambridge: Cambridge International Science Publishing; 1995.
- [32] Satya Prasad VV, Khaple S, Baligidad RG. Melting, processing, and properties of disordered Fe–Al and Fe–Al–C based alloys. *JOM* 2014.
- [33] Case SL, Van Horn KR. *Aluminum in Iron and Steel*. New York: Wiley; 1953.
- [34] Yang M, Akiyama Y, Sasaki T. Evaluation of change in material properties due to plastic deformation. *J Mat Process Technol* 2004.
- [35] Davis CL, Mukhopadhyay P, Strangwood M, Potter M, Dixon S, Morris PF. Comparison between elastic modulus and ultrasonic velocity anisotropy with respect to rolling direction in steels. *Ironmaking Steelmaking* 2008.
- [36] Granato A, Hikata A, Lücke K. Recovery of damping and modulus changes following plastic deformation. *Acta Metall* 1958.
- [37] Herrmann J, Inden G, Sauthoff G. Deformation behaviour of iron-rich iron-aluminium alloys at low temperatures. *Acta Mater* 2003.
- [38] Morris DG, Munoz-Morris MG, Requejo LM. Work hardening in Fe–Al alloys. *Mater Sci Eng. A* 2007.
- [39] Falat L, Schneider A, Sauthoff G, Frommeyer G. Constitution and microstructures of Fe–Al–M–C (M= Ti, V, Nb, Ta) alloys with carbides and Laves phase. *Intermetallics* 2005.
- [40] Castan C, Montheillet F, Perlade A. Dynamic recrystallization mechanisms of an Fe–8% Al low density steel under hot rolling conditions. *Scripta Mater* 2013.
- [41] Rana R, Liu C, Ray RK. Low-density low-carbon Fe–Al ferritic steels. *Scripta Mater* 2013.
- [42] Brück U, Frommeyer G, Jimenez J. Light-weight steels based on iron-aluminium: Influence of micro alloying elements (B, Ti, Nb) on microstructures, textures and mechanical properties. *Steel Res Int* 2012.
- [43] Zargarán A, Kim H, Kwak JH, Kim NJ. Effects of Nb and C additions on the microstructure and tensile properties of lightweight ferritic Fe–8Al–5Mn alloy. *Scripta Mater* 2014.
- [44] Rana R, Liu C, Ray RK. Evolution of microstructure and mechanical properties during thermomechanical processing of a low-density multiphase steel for automotive application. *Acta Mater* 2014.

- [45] Han SY, Shin SY, Lee S, Kim NJ, Kwak JH, Chin KG. Effect of carbon content on cracking phenomenon occurring during cold Rolling of three light-weight steel plates. *Metall Mater Trans A* 2010.
- [46] Sohn SS, Lee BJ, Lee S, Kwak JH. Effect of Mn addition on microstructural modification and cracking behaviour of ferritic light-weight steels. *Metall Mater Trans A* 2014.
- [47] Sohn SS, Lee BJ, Lee S, Kwak JH. Effects of aluminium content on cracking phenomenon occurring during cold rolling of three ferrite-based lightweight steel. *Acta Mater* 2013.
- [48] Shin SY, Lee H, Han SY, Seo CH, Choi K, Lee S, et al. Correlation of microstructure and cracking phenomenon occurring during hot rolling of lightweight steel plates. *Metall Mater Trans A* 2010.
- [49] Sohn SS, Lee BJ, Lee S, Kim NJ, Kwak JH. Effect of annealing temperature on microstructural modification and tensile properties in 0.35C–3.5Mn–5.8Al lightweight steel. *Acta Mater* 2013.
- [50] Seo CH, Kwon KH, Choi K, Kim KH, Kwak JH, Leed S, et al. Deformation behaviour of ferrite–austenite duplex lightweight Fe–Mn–Al–C steel. *Scripta Mater* 2012.
- [51] Sohn SS, Choi K, Kwak JH, Kim NJ, Lee S. Novel ferrite–austenite duplex lightweight steel with 77% ductility by transformation induced plasticity and twinning induced plasticity mechanisms. *Acta Mater* 2014.
- [52] Lee S, Jeong J, Lee YK. Precipitation and dissolution behaviour of j-carbide during continuous heating in Fe-9.3Mn-5.6Al-0.16C lightweight steel. *J Alloys Compd* 2015.
- [53] Jeong J, Lee CY, Park IJ, Lee YK. Isothermal precipitation behaviour of j-carbide in the Fe–9Mn–6Al–0.15C lightweight steel with a multiphase microstructure. *J Alloys Compd* 2013.
- [54] Park SJ, Hwang B, Lee KH, Lee TH, Suh DW, Han HN. Microstructure and tensile behaviour of duplex low-density steel containing 5 mass% aluminium.
- [55] Rigaut V, Daloz D, Drillet J, Perlade A, Maugis P, Lesoult G. Phase equilibrium study in quaternary iron-rich Fe–Al–Mn–C alloys.
- [56] Cai Z, Ding H, Ying Z, Misra RDK. Microstructural evolution and deformation behaviour of a hot-rolled and heat-treated Fe-8Mn-4Al-0.2C steel. *J Mater Engg.*
- [57] Sohn SS, Song H, Kim JG, Kwak JH, Kim HS, Lee S. Effects of annealing treatment prior to cold rolling on delayed fracture properties in ferrite-austenite duplex lightweight steels. *Metall Mater.*
- [58] Han SY, Shin SY, Lee HJ, Lee BJ, Lee S, Kim NJ, et al. Effects of annealing temperature on microstructure and tensile properties in ferritic lightweight steels. *Metall Mater Trans A* 2012.
- [59] Seol JB, Raabe D, Choi P, Park HS, Kwak JH, Park CG. Direct evidence for the formation of ordered carbides in a ferrite-based low-density Fe–Mn–Al–C alloy studied by transmission electron microscopy and atom probe tomography. *Scripta Mater* 2013.
- [60] Sohn SS, Song H, Suh BC, Kwak JH, Lee BJ, Kim NJ, et al. Novel ultra-high-strength (ferrite + austenite) duplex light weight steels achieved by fine dislocation substructures (Taylor lattices), grain refinement, and partial recrystallization. *Acta Mater* 2015.
- [61] Yang MX, Yuan FP, Xie QG, Wang YD, Ma E, Wu XL. Strain hardening in Fe-16Mn-10Al-0.86C-5Ni high specific strength steel.
- [62] Wu ZQ, Ding H, Li HY, Huang ML, Cao FR. Microstructural evolution and strain hardening behaviour during plastic deformation of Fe–12Mn–8Al–0.8C steel. *Mater Sci Engg.*

- [63] Hwang SW, Ji JH, Lee EG, Park KT. Tensile deformation of a duplex Fe–20Mn–9Al–0.6C steel having the reduced specific weight. *Mater Sci Eng. A* 2011.
- [64] Yang F, Song R, Li Y, Sun T, Wang K. Tensile deformation of low-density duplex Fe–Mn–Al–C steel.
- [65] Zhang L, Song R, Zhao C, Yang F. Work hardening behaviour involving the substructural evolution of an austenite–ferrite Fe–Mn–Al–C steel. *Mater Sci Engg.*
- [66] Zhao C, Song R, Zhang L, Yang F, Kang T. Effect of annealing temperature on the microstructure and tensile properties of Fe–10Mn–10Al–0.7C low-density steel. *Mater Des* 2016.
- [67] Zhang L, Song R, Zhao C, Yang F, Xu Y, Peng S. Evolution of the microstructure and mechanical properties of an austenite–ferrite Fe–Mn–Al–C steel. *Mater Sci Eng. A* 2015.
- [68] Ha MC, Koo JM, Lee JK, Hwang SW, Park KT. Tensile deformation of a low-density Fe–27Mn–12Al–0.8C duplex steel in association with ordered phases at ambient temperature. *Mater Sci Eng. A* 2013.
- [69] Rana R, Loiseaux J, Lahaye C. Microstructure, mechanical properties and formability of a duplex steel. *Mater Sci Forum* 2012.
- [70] Etienne A, Massardier-Jourdan V, Cazottes S, Garat X, Soler M, Zuazo I, et al. Ferrite effects in Fe-Mn-Al-C triplex steels. *Metall Mater Trans A* 2014.
- [71] You RK, Kao PW, Gan D. Mechanical properties of Fe-30Mn-10Al-1C-1Si alloy. *Mater Sci Eng. A* 1989.
- [72] Hwang SW, Ji JH, Park KT. Effects of Al addition on high strain rate deformation of fully austenitic high Mn steels. *Mater Sci Eng.* 2011.
- [73] Chang SC, Hsiau YH, Jahn MT. Tensile and fatigue properties of Fe-Mn-Al-C alloys. *J Mater Sci* 1989.
- [74] Gau YJ, Wu JK. The influence of alloying elements on the corrosion behaviour of Fe-Mn-Al alloys. *Corr Prevent Cont* 1997.
- [75] Tuan YH, Wang CS, Tsai CY, Chao CG, Liu TF. Corrosion behaviours of austenitic Fe–30Mn–7Al–xCr–1C alloys in 3.5% NaCl solution. *Mater Chem Phys* 2009.
- [76] Wang CS, Tsai CY, Chao CG, Liu TF. Effect of chromium content on corrosion behaviours of Fe-9Al-30Mn-(3,5,6.5,8) Cr-1C alloys. *Mater Trans* 2007.
- [77] Lee JW, Wu CC, Liu TF. The influence of Cr alloying on microstructures of Fe–Al–Mn–Cr alloys. *Scripta Mater* 2005.
- [78] Huang CF, Ou KL, Chen CS, Wang CH. Research of phase transformation on Fe–8.7Al–28.3Mn–1C–5.5Cr alloy. *J Alloys Compd* 2009.
- [79] Tjong SC, Wu CS. The microstructure and stress corrosion cracking behaviour of precipitation-hardened Fe-8.7Al-29.7Mn-1.04C alloy in 20% NaCl solution. *Mater Sci Eng.* 1986.
- [80] Chang SC, Liu JY, Juang HK. Environment-assisted cracking of Fe-32%Mn-9%Al alloys in 3.5% sodium chloride solution. *Corrosion.*
- [81] Ku JS, Ho NJ, Tjong SC. Properties of electron-beam-welded and laser-welded austenitic Fe-28Mn-5Al-1C alloy. *J Mater Sci.*

[82] Tjong SC, Zhu SM, Ho NJ, Ku JS. Solidification microstructure and creep rupture behaviour of electron beam welded austenitic Fe-28M-6Al-1C alloys.